Since January 2020 Elsevier has created a COVID-19 resource centre with free information in English and Mandarin on the novel coronavirus COVID-19. The COVID-19 resource centre is hosted on Elsevier Connect, the company's public news and information website.

THE JOURNAL OF BIOLOGICAL CHEMISTRY
Vol. 279, No. 11, Issue of March 12, pp. 10136–10141, 2004
Printed in U.S.A.

Coronavirus Replication Complex Formation Utilizes Components of Cellular Autophagy*

Received for publication, June 10, 2003, and in revised form, December 11, 2003
Published, JBC Papers in Press, December 29, 2003, DOI 10.1074/jbc.M306124200

Erik Prentice,[a,b] W. Gray Jerome,[c,d] Tamotsu Yoshimori,[e,f] Noboru Mizushima,[g,h] and Mark R. Denison[a,b,i,j]

From the Departments of [a]Microbiology and Immunology, [i]Pediatrics, [c]Pathology, and [d]Cancer Biology and the [b]Elizabeth B. Lamb Center for Pediatric Research, Vanderbilt University Medical Center, Nashville, Tennessee 37221, [e]Department of Cell Genetics, National Institute of Genetics, Mishima 411-8540, Japan, [g]Department of Cell Biology, National Institute for Basic Biology, Okazaki 444-8585, Japan, [h]Unit Process and Combined Circuit, Precursory Research for Embryonic Science and Technology, Japan Science and Technology Corporation, and [f]Core Research for Evolutionary Science and Technology Program, Japan Science and Technology Corporation, Kawaguchi 332-0012, Japan

The coronavirus mouse hepatitis virus (MHV) performs RNA replication on double membrane vesicles (DMVs) in the cytoplasm of the host cell. However, the mechanism by which these DMVs form has not been determined. Using genetic, biochemical, and cell imaging approaches, the role of autophagy in DMV formation and MHV replication was investigated. The results demonstrated that replication complexes co-localize with the autophagy proteins, microtubule-associated protein light-chain 3 and Apg12. MHV infection induces autophagy by a mechanism that is resistant to 3-methyladenine inhibition. MHV replication is impaired in autophagy knockout, *APG5−/−*, embryonic stem cell lines, but wild-type levels of MHV replication are restored by expression of Apg5 in the *APG5−/−* cells. In MHV-infected *APG5−/−* cells, DMVs were not detected; rather, the rough endoplasmic reticulum was dramatically swollen. The results of this study suggest that autophagy is required for formation of double membrane-bound MHV replication complexes and that DMV formation significantly enhances the efficiency of replication. Furthermore, the rough endoplasmic reticulum is implicated as the possible source of membranes for replication complexes.

Autophagy is a cellular stress response that functions to recycle proteins and organelles (1, 2). The mechanism of autophagy has been extensively studied in yeast, with more than 15 genes identified that are required for functional autophagy (1, 2). Autophagy has been most widely studied as a response to amino acid starvation; however, the role that autophagy may play in development, disease pathogenesis, and microbial infections is only beginning to be examined. Studies with Sindbis virus and herpes simplex virus-1 have demonstrated that autophagy may be an important defense mechanism against infection with those viruses (3, 4).

Cellular autophagy has been proposed to be a mechanism of replication complex formation for the positive sense RNA viruses, poliovirus, equine arteritis virus, and mouse hepatitis virus (MHV)[1] (5–8). For all of these viruses, replication complexes have been shown to form as double membrane vesicles (DMVs) in the cytoplasm, which is suggestive of an autophagic origin. For poliovirus and MHV, multiple organelle markers have been reported to co-localize or co-fractionate with replication complexes, also consistent with an autophagy-like process (6, 7, 9, 10). In addition, poliovirus and MHV replication complexes have been reported to acquire lysosomal markers over the course of infection similar to the maturation of autophagosomes. These studies have demonstrated that replication complexes formed by these viruses share features of autophagosomes; however, it is not known whether cellular autophagy is required for the formation of replication complexes. Recently, markers for autophagic vacuoles in mammalian cells have been described: microtubule-associated protein light chain 3 (LC3) and Apg12 (14, 15). In addition, murine embryonic stem (ES) cells lacking a critical gene product in the pathway of cellular autophagy (Apg5) have been established (12). Together, these advances provide new approaches to investigating the role of cellular autophagy in viral infections.

Coronaviruses are enveloped positive sense RNA viruses that replicate entirely in the cytoplasm of cells. Coronaviruses are important causes of disease in many domesticated animals and are responsible for up to 30% of human colds. In addition, a newly recognized human coronavirus has recently been identified as the causative agent of severe acute respiratory syndrome (SARS) (13–15). Coronaviruses and arteriviruses are the two families within the order Nidovirales. Viruses in this order have similar genome organization and express the proteins required for RNA replication as polyproteins (5, 9, 16–23). Thus, studies of the mechanisms of coronavirus replication complex formation may be critical to understanding the pathogenesis, treatment, and prevention of coronavirus infections.

MHV is the prototype coronavirus for studies of replication complex formation and function. MHV replication complexes

* This work was supported by Public Health Service Grant AI50083 (to M. R. D.) and National Institutes of Health Training Grant 5 T32 HL07751 in mechanisms of vascular disease (to E. P.). Experiments were performed in part through the use of the VUMC Cell Imaging Core Resource (supported by National Institutes of Health Grants CA68485 and DK20593). The costs of publication of this article were defrayed in part by the payment of page charges. This article must therefore be hereby marked "*advertisement*" in accordance with 18 U.S.C. Section 1734 solely to indicate this fact.

[j] To whom correspondence should be addressed: Dept. of Pediatrics, Vanderbilt University Medical Ctr., D6217 MCN, Nashville, TN 37232-2581. Tel.: 615-343-9881; Fax: 615-343-9723; E-mail: mark.denison@vanderbilt.edu.

[1] The abbreviations used are: MHV, mouse hepatitis virus; DMV, double membrane vesicles; 3-MA, 3-methyladenine; LC3, light chain 3 (microtubule-associated protein); ES, embryonic stem; SARS, severe acute respiratory syndrome; CoV, coronavirus; p.i., postinfection; DBT, delayed brain tumor; N, nucleocapsid; M, membrane; hel, helicase; pfu, plaque-forming unit; DMEM, Dulbecco's modified Eagle's medium; FCS, fetal calf serum; PBS, phosphate-buffered saline; BSA, bovine serum albumin; ER, endoplasmic reticulum; RER, rough endoplasmic reticulum.

form in the cytoplasm of infected cells and are first detectable at 4–5 h p.i. by immunofluorescence in MHV-infected delayed brain tumor (DBT) cells (9, 22, 24, 25). Replication complexes appear as punctate perinuclear foci, with the number and size of replication complexes increasing over the course of infection (9, 22, 24–26). These complexes are active in viral RNA synthesis and contain all replicase proteins tested to date, as well as the structural nucleocapsid (N) protein (9, 22, 24, 25). We have shown previously that components of the replication complex, the helicase (hel) and N proteins, translocate between 6 and 8 h p.i. from sites of RNA replication to sites of viral assembly in the ER-Golgi intermediate compartment (25).

In this study, we sought to determine whether cellular autophagy was induced by, and required for, MHV replication complex formation and viral replication. Cell imaging and biochemical and genetic approaches were used to demonstrate that MHV replication complexes were associated with the autophagic markers LC3 and Apg12 and that MHV proteins known to translocate away from replication complexes also lost their association with LC3 over time. Furthermore, MHV infection induced autophagy, and inhibition of autophagy inhibited MHV growth. These results indicate that the process of autophagy plays an important role in the replication of MHV.

EXPERIMENTAL PROCEDURES

Viruses, Cells, and Starvation—MHV, strain A59, was used for infections throughout this study. All infections were performed at a multiplicity of infection of 10 plaque-forming units/cell (pfu/cell) unless otherwise indicated. DBT cells were used in LC3 localization, translocation studies, and long-lived protein degradation experiments (27, 28). For this report, italicized capitalized nomenclature (*e.g. APG5*) refers to the gene, whereas an initial capital letter followed by lowercase lettering (*e.g.* Apg5) refers to the protein. *APG5* was knocked out in A11 and B22 cells by targeted homologous recombination of the *APG5* locus in R1 parental ES cells and were generated as described previously (12). The *APG5* cDNA was cloned into pCI-neo (Promega), and stable *APG5* transformants (WT13) were created by genomic integration of the plasmid into *APG5*−/− ES cells (A11) (12). ES cells were maintained on gelatinized 60-mm dishes in complete ES medium (high glucose Dulbecco's modified Eagle's medium (DMEM) supplemented with 20% fetal calf serum (FCS), 2 mM L-glutamine, nonessential amino acids (Invitrogen), 1 μM 2-mercaptoethanol, antibiotics, and 1000 units/ml leukemia inhibitory factor (Chemicon, Inc.).

Long-lived Protein Degradation Assay—Measurement of long-lived protein degradation was performed as described previously (3). Results are of representative experiments performed in triplicate ± S.D. Briefly, DBT cells were labeled for 72 h in medium containing 65 μM concentrations of unlabeled leucine and [^{3}H]leucine (1 μCi/ml). The cells were then washed and incubated in medium containing excess cold leucine (2 mM) for 24 h to allow for degradation of short-lived proteins. These labeled cells were then infected, amino acid starved, or maintained in 10% FCS-containing DMEM. At 0, 4, and 8 h after infection or starvation, media supernatants were analyzed for acid-soluble radioactivity. Total trichloroacetic acid-precipitable radioactivity of the cell monolayers was assayed at the end of the time course, and the percentage of long-lived protein degradation at each time point was determined by the formula: % degradation = (^{3}H counts at time point/sum of ^{3}H counts at each time point + total cell-associated radioactivity) × 100.

Viral Growth Analysis—All results presented are of experiments performed in triplicate, with each experiment being assayed in duplicate. Error bars represent 1 standard deviation. T75 flasks of cells were infected with MHV at a multiplicity of infection of 0.1 pfu/cell, and the virus was allowed to adsorb at room temperature for 1 h. The inoculum was removed, and the cells were washed three times with pre-warmed PBS before being overlaid with 10 ml of the appropriate medium (DMEM, 10% FCS for DBT cells, ES cell medium for all other cells). 250-μl samples of media were removed at 1, 4, 10, 16, 24, and 32 h p.i. with replacement of 250 μl of media at each time point. The amount of virus in the media at each time point was quantitated by plaque assay. The results represent viral yield, which is defined as peak titer/input titer, and have been adjusted for differences in cell numbers between cell types. 24 h p.i. represented the time of peak titer in all experiments.

Antibodies—The B1 (αhel) and αp1a-22 antibodies have been described previously (22, 24). The αM (J.1.3) and αN (J.3.3) mouse monoclonal antibodies were provided by John Fleming (University of Wisconsin, Madison, WI). The LC3, Apg5, and Apg12 antibodies were generated in rabbits as described previously (29, 30). The antibody against β-tubulin was purchased from Sigma.

Western Blotting—Whole-cell lysates were prepared with a lysis buffer (2% Nonidet P-40, 0.2% SDS in PBS with protease inhibitors). Western blotting was performed as described previously (12).

Immunofluorescence—For immunofluorescence experiments, DBT cells were plated on glass coverslips. Infections were performed at a multiplicity of infection = 10 pfu/cell at 37 °C in DMEM containing 10% FCS. The inoculum was removed at 1 h p.i., and the cells were washed three times with pre-warmed DMEM and replaced with DMEM containing 10% FCS. At the times indicated, the cells were washed once with Tris-HCl, pH 7.4, and fixed and permeabilized by the addition of −20 °C 100% methanol. The cells were rehydrated in PBS containing 5% bovine serum albumin (BSA). For dual labeling experiments, in which one primary antibody was derived from mouse and the other from rabbit, the primary antibodies were combined in a diluent containing PBS, 2% goat serum, 0.05% Nonidet P-40, and 1% BSA. Antibodies were allowed to adsorb for 1 h at room temperature and then washed twice with PBS, 0.05% Nonidet P-40, and 1% BSA. The cells were then incubated for 1 h at room temperature with a 1:1000 dilution of anti-rabbit and/or anti-mouse secondary antibodies conjugated to Alexa 488 or Alexa 546 (Molecular Probes, Eugene, OR). The cells were washed twice with PBS, 0.05% Nonidet P-40, and 1% BSA and then once with PBS prior to being rinsed in deionized H_2O and mounted onto glass slides with Aquapolymount (Polysciences, Inc.). For the p22/LC3 dual label experiment, in which both primary antibodies were generated in rabbits, anti-p22 was purified and directly conjugated to a fluorescent dye (Alexa 488). Staining for LC3 was performed as above. Following LC3 staining, conjugated anti-p22 was diluted 1:50 in PBS, 2% goat serum, 0.05% Nonidet P-40, and 1% BSA and allowed to adsorb for 1 h at room temperature. The cells were then washed twice with PBS, 0.05% Nonidet P-40, and 1% BSA, once with PBS, and once with deionized H_2O prior to mounting. Immunofluorescence was detected at 488 and 543 nm using a 40× oil-immersion objective (numerical aperture = 1.3) on a Zeiss 510 laser scanning microscope.

Quantitation of Protein Co-localization—Immunofluorescence images were acquired with maximal dynamic range. For each protein pair and time point, 10 fields of view were acquired and processed for co-localization measurement. The average number of infected cells/field was five. Images were exported to MetaMorph software (Universal Imaging) for quantitative analysis of fluorescence. In MetaMorph, images were split into the red and green channels. A background threshold had been determined for these experiments by application of anti-p22 to mock-infected DBT cells and processing with the appropriate secondary antibody. The resulting detected fluorescence was considered background, and the lower limit threshold was set to exclude pixels below that level. The upper limit threshold was set to exclude saturated pixels. Co-localization measurements were then performed on the images, and the resultant data was exported to Microsoft Excel for generation of time course graphs.

Electron Microscopy—DBT, R1, A11, and WT cells were mock-infected, infected for 6 h, or starved for 2 h, and then washed once with 0.1 M cacodylate buffer, pH 7.4. The cells were fixed with 2.5% glutaraldehyde in cacodylate buffer at 37 °C for 1 h and then overnight at 4 °C. Cell pellets were then postfixed with 1% OsO_4 in cacodylate buffer for 1 h at room temperature and dehydrated stepwise with ethanol. The dehydrated pellets were rinsed with propylene oxide for 30 min at room temperature and then embedded in Spurr resin for sectioning. Images of thin sections were acquired using a CM-12 microscope running at 80 keV.

RESULTS

Replicase Proteins Co-localize with Markers for Autophagic Vacuoles—To determine whether MHV replication complexes were forming on the surface of autophagosomes, the subcellular localization of replication complexes and markers for autophagic vacuoles, microtubule-associated protein 1 LC3 and Apg12, were compared by immunofluorescence laser scanning confocal microscopy in MHV-infected DBT cells (29). In mock-infected DBT cells, LC3 was detected as small discrete foci distributed throughout the cell cytoplasm (Fig. 1*A*). When DBT cells were infected with MHV, some LC3 was concentrated in larger foci. The coalescence of LC3 into larger complexes has

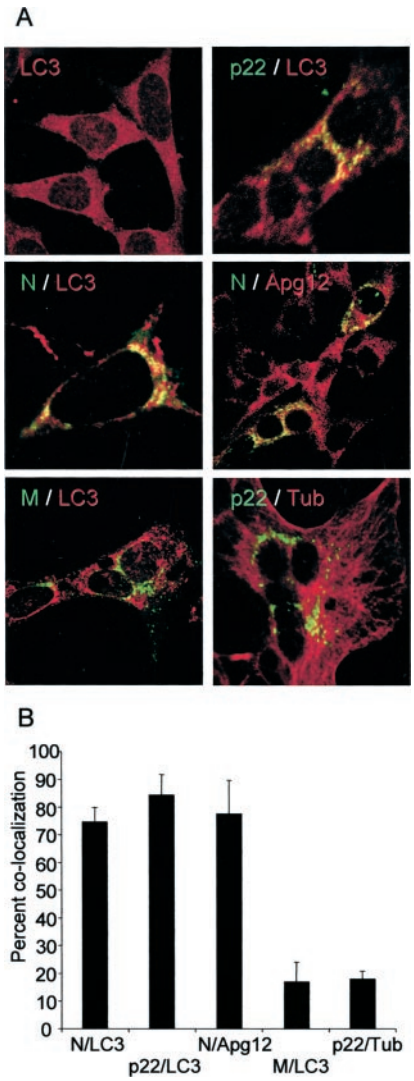

FIG. 1. **Replicase proteins co-localize with markers for autophagy.** *A*, DBT cells were infected with MHV for 6 h and then fixed and processed for immunofluorescence. Cells were probed with antibodies against LC3, Apg12, β-tubulin, N, p22, and M. The localization of LC3 and β-tubulin (*red*, all panels) was compared with N, p22, and M (*green*, as labeled in panels), with *yellow* pixels indicating areas of co-localization. *B*, quantitation of fluorescence co-localization. The percent co-localization of the indicated proteins was determined as described under "Experimental Procedures."

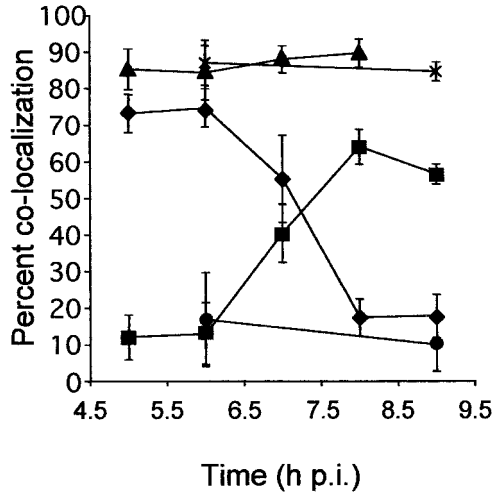

FIG. 2. **The hel and N proteins translocate away from LC3-positive membranes to sites of assembly over the course of infection.** MHV-infected DBT cells were harvested from 5 to 9 h p.i. Quantitative analysis of co-localization was performed for the indicated protein pairs. P22 and LC3 (*triangles*) were 85% co-localized throughout infection. Hel and N (*stars*) were 85% co-localized throughout infection. N and LC3 co-localization (*diamonds*) decreased over the course of infection from 75% at 5 and 6 h p.i. to 18% at 8 and 9 h p.i. Hel and M co-localization (*squares*) increased from 12% at 5 h p.i. to 60% by 8h p.i. M and LC3 (*circles*) were <18% co-localized throughout infection.

been shown previously to correspond to association of LC3 with autophagic vacuoles (29). When MHV-infected cells were probed at 6 h p.i. for LC3 and MHV proteins known to localize to replication complexes (p22 and N), both p22 and N co-localized with a subset of LC3-positive foci (Fig. 1*A*). Quantitation of co-localization showed that N and LC3 were 75% co-localized, whereas p22 and LC3 were 84% co-localized (Fig. 1*B*). Significantly, p22 and N were co-localized primarily with the larger foci of LC3 accumulation that were characteristic of autophagosomes. N was 77% co-localized with Apg12, a protein demonstrated to localize to autophagic isolation membranes (Fig. 1). Thus, MHV replication complexes were associated with two independent protein markers for autophagic membranes.

To determine whether the co-localization with autophagosomal markers was specific to replication complexes, the localization of LC3 was compared with the MHV membrane (M) protein. LC3 and M (which is known to target to sites of virus assembly in the ER-Golgi intermediate compartment and Golgi) were 17% co-localized, demonstrating that LC3 was not significantly associated with membranes derived from Golgi or ER-Golgi intermediate compartment or with sites of virus assembly (Fig. 1). LC3 has also been reported to be associated with microtubules. However, not all of the LC3 in an infected cell co-localized with replication complexes. Thus, to determine whether replication complexes and the replication complex-associated LC3 were associated with microtubules, we compared the localization of MHV-p22 to β-tubulin in MHV-infected cells. β-Tubulin was only 18% co-localized with p22, indicating that the majority of replication complexes and LC3 were not associated with microtubules (Fig. 1).

LC3 Remains Associated with Replication Complexes throughout Infection—Having shown that replication complexes co-localized with LC3, we next determined if LC3 remained associated with replication complexes throughout the course of infection. The co-localization of LC3, hel, N, p22, and M was determined quantitatively at 5, 6, 7, 8, 9, and 10 h p.i. At 5 and 6 h p.i., hel and M were 12 and 13% co-localized, but by 7 h p.i., the two proteins were 40% co-localized, and by 8 h p.i., hel and M were 64% co-localized. When the localization of the hel and N proteins were compared, hel and N were >85% co-localized throughout the infection (Fig. 2). Together, these results provided quantitative confirmation of previous observations demonstrating that the hel and N proteins translocate away from replication complexes to sites of viral assembly, possibly to deliver newly synthesized RNA nucleocapsids for integration into newly forming virions (25).

When LC3 localization was compared with N and M at 5 and 6 h p.i., N and LC3 were 74% co-localized, but by 7 h p.i., N and LC3 were only 55% co-localized and by 8 and 9 h p.i. were only 17% co-localized. When the localization of LC3 and M were compared, LC3 and M were <18% co-localized throughout the course of the infection (Fig. 2). Thus, LC3 did not translocate with hel and N to sites of assembly. To confirm that LC3 remained associated with replication complexes, the localization of LC3 was compared with the replication complex-associated protein, p22 (25). LC3 and p22 remained 85% co-localized throughout the course of infection (Fig. 2). These experiments demonstrated that LC3 did not change localization over time

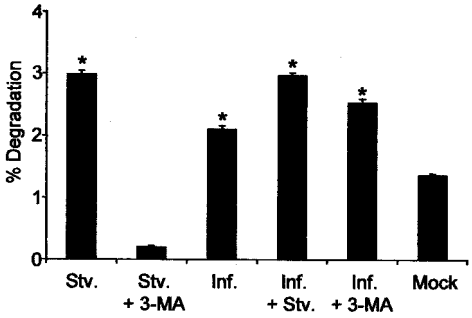

FIG. 3. **Long-lived protein degradation assay in DBT cells.** DBT cells were treated as labeled. Data represent the amount of protein degraded over an 8-h time course. The amount of long-lived protein degradation was determined as described under "Experimental Procedures." *Asterisks* denote statistically significant values.

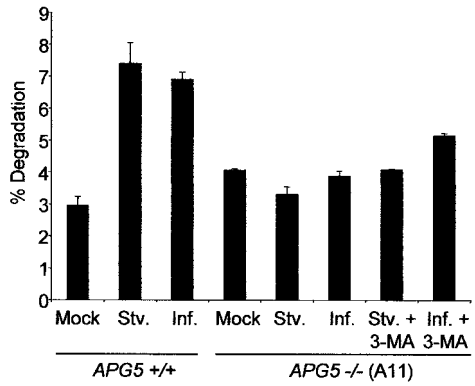

FIG. 4. **Long-lived protein degradation assay in *APG5*+/+ and *APG5*−/− cells.** R1 (*APG5*+/+) and A11 (*APG5*−/−) cells were treated as labeled, and long-lived protein degradation levels were determined as described under "Experimental Procedures." Data represent the amount of protein degraded over an 8-h time course.

but remained associated with proteins in viral replication complexes.

Autophagy Is Induced by MHV Infection—The co-localization of replicase proteins with LC3 suggested that replication complexes were forming on autophagic vacuoles. A possible mechanism for targeting of replicase proteins to autophagic vacuoles would be the specific induction of cellular autophagy by MHV. The rate of degradation of long-lived proteins is a well characterized method shown to provide an accurate measure of the level of autophagy in cells (1, 3, 12). To determine whether MHV infection induced autophagy, the rate of long-lived protein degradation was determined in DBT cells that were either amino acid-starved, MHV-infected, starved and MHV-infected, or incubated with normal media (Fig. 3). DBT cells that were starved increased their long-lived protein degradation from 1.2 to 2.9% ($p < 0.0001$, Student's t test) compared with DBT cells incubated with normal media. In MHV-infected cells, protein degradation was significantly increased to 2.1% ($p < 0.0006$, Student's t test) over control cells, and when cells were both starved and infected, protein degradation was increased to 2.9% ($p < 0.0001$, Student's t test) compared with control cells.

When cells were starved in the presence of the autophagy inhibitor 3-methyladenine (3-MA), the increase in protein degradation was blocked. In contrast, long-lived protein degradation increased to 2.6% ($p < 0.0001$, Student's t test) in 3-MA-treated infected cells, demonstrating that MHV-induced protein degradation was 3-MA insensitive (Fig. 3). 3-MA did inhibit MHV growth in a dose-dependant manner (data not shown). However, 3-MA is a nucleoside analog that may interfere with viral RNA replication and transcription. Nevertheless, our results suggest that MHV induced autophagy via a unique pathway or was able to complement the 3-MA-inhibited steps resulting in functional autophagy.

To determine whether an intact autophagic pathway was required for the MHV-induced stimulation of long-lived protein degradation, analysis of long-lived protein degradation was performed in murine embryonic stem cell lines expressing Apg5 (R1) or in *APG5* knockout (A11) cells under the conditions used for DBT cells. The knockout of *APG5* has been shown to prevent the formation of autophagic vacuoles (12). Furthermore, these cells were shown to have reduced rates of degradation of long-lived proteins (12, 31, 32).

When R1 cells were starved or infected with MHV, long-lived protein degradation rates were 7.5% and 7.1%, respectively (Fig. 4). In contrast, when A11 cells were starved, infected, or starved and infected, there was no change in levels of protein degradation compared with mock-infected cells (Fig. 4). When 3-MA was added to starved or infected A11 cells, no change in protein degradation was observed compared with mock-infected cells (Fig. 4). Thus, an intact autophagic signaling pathway appears to be required for MHV-induced protein degradation.

MHV Replication Is Decreased in the Absence of APG5—Having demonstrated that MHV infection induced autophagy and that MHV replication complexes contained markers for autophagic vacuoles, we next determined whether autophagy was required for MHV replication. MHV growth was compared in ES cell lines that were *APG5*+/+ (R1) and *APG5*−/− (A11, B22) and in ES cells that were *APG5*−/− but reconstituted by Apg5 expression from stably integrated *APG5* plasmid (WT13). To demonstrate that Apg5 was expressed in R1 and WT13 but not in the A11 or B22 cell lines, Western blot analysis with Apg12 and Apg5 antibodies was performed. It has been shown previously that nearly all Apg5 and Apg12 is detected as a 56-kDa Apg12-Apg5 conjugate, and that detection of a 56-kDa band is an accurate representation of the level of Apg5 expression in a given cell line (12). Western blotting with antibodies to Apg12 revealed the presence of the 56-kDa Apg5-Apg12 conjugate in the R1 and WT13 cells but not in the A11 or B22 cells (Fig. 5*A*). When the membrane was stripped and reprobed with antibodies against Apg5, 56-kDa proteins were again detected in the R1 and WT13 lanes, but not in the A11 or B22 lanes (Fig. 5*B*). The levels of Apg5 expression in wild-type R1 and Apg5-reconstituted WT13 cells were equivalent. Having experimentally confirmed that Apg5 was expressed in R1 and WT13 cells and not expressed in A11 and B22 cells, these cells were then used to determine whether defects in autophagy impacted the ability of MHV to grow. Viral yield following MHV infection of in R1 cells was 6.35 ± 0.10 log pfu/ml at 24 h p.i. (Fig. 5*C*). MHV grew to 2.15 ± 0.96 log pfu/ml and 2.62 ± 0.19 log pfu/ml at 24 h p.i. in the B22 and A11 *APG5*−/− cell lines, respectively, a decrease of >99.99%. Reconstitution of the *APG5* knockout by plasmid expression of *APG5* increased viral yield to 5.90 ± 0.07 log pfu/ml, demonstrating that the inhibition of MHV replication seen in the A11 and B22 cell lines was because of the lack of Apg5 expression and that the defect could be complemented by expression of Apg5.

MHV-induced DMV Formation Requires Autophagy—The above results demonstrated that functional autophagy was critical for wild-type levels of MHV replication. To determine whether formation of DMVs was linked to autophagy in MHV-infected cells, electron micrographs were obtained of MHV-infected autophagy-incompetent A11 cells. In mock-infected A11 cells, a minor swelling of rough endoplasmic reticulum (RER) was seen, but normal membrane morphology was otherwise observed (Fig. 6). In the autophagy-competent R1 cells,

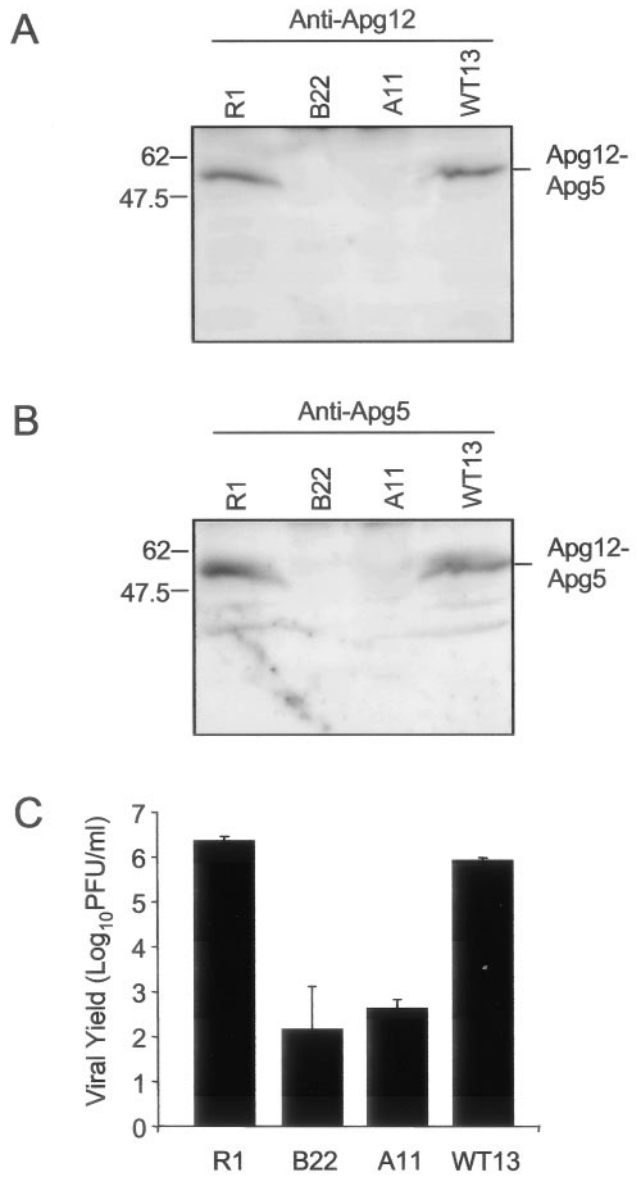

FIG. 5. **MHV growth is decreased in autophagy-deficient cells.** *A*, Western blot analysis of R1 (*APG5*+/+), A11 (*APG5*−/−), B22 (*APG5*−/−), and WT13 (*APG5*−/− + *APG5* plasmid) cells with Apg12 antibody. *B*, Western blot analysis of R1 (*APG5*+/+), A11 (*APG5*−/−), B22 (*APG5*−/−), and WT13 (*APG5*−/− with *APG5* plasmid) cells with Apg5 antibody. *C*, the indicated cells were infected with MHV, and virus growth was determined by plaque assay.

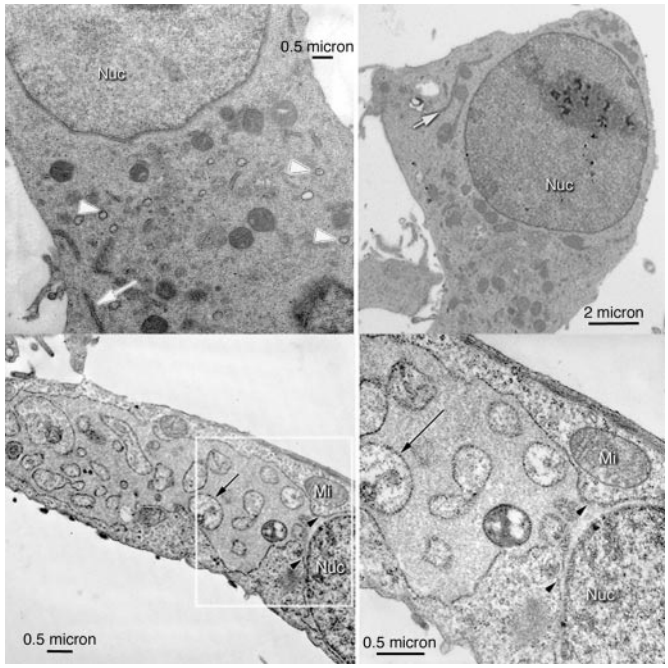

FIG. 6. **Electron micrographs of infected R1 cells and infected and mock-infected A11 cells.** Infected R1 cells (*APG5*+/+) do not show a swollen ER phenotype (*white arrow*) but instead are filled with viral replication complexes (*white arrowheads*, *top left panel*). Mock-infected A11 cells (*top right panel*) appeared morphologically normal, with minor swelling of the rough ER (*white arrow*) occasionally detected. MHV-infected A11 cells contained extremely swollen interconnected areas of RER that appear to surround cytoplasmic regions to form vesicles (*bottom left panel*). The *lower right panel* shows a higher magnification view of swollen RER (*black arrow* points to same vesicle in *both panels*). The *black arrowheads* indicate an area of membrane confluence with the outer nuclear membrane (*bottom right panel*). *Mi*, mitochondrion; *Nuc*, nucleus.

MHV infection resulted in the development of DMVs similar to those seen in other MHV-infected cells (Fig. 6). In contrast, despite the demonstrated ability of MHV to replicate in A11 cells, DMVs were not detected in the MHV-infected A11 cells. Instead, the morphology of the membranes in MHV-infected autophagy-incompetent A11 cells was impressively deranged, with hyper-swollen membranes detected throughout the majority of cells (Fig. 6). These membranes had continuity with the nuclear envelope and decoration with ribosomes, strongly suggesting an origin in the RER. When viewed in sagittal section, multiple large vesicles appeared to be surrounded by the swollen ER (Fig. 6). Also present were large swollen structures with loosely approximated second membranes that had the appearance of early autophagic vacuoles. The changes observed in MHV-infected A11 cells were entirely absent in R1 or DBT cells under any conditions, demonstrating that the membrane changes were induced by MHV infection.

DISCUSSION

The findings in this report demonstrate that cellular autophagy plays an important role in MHV replication and that infection with MHV induces cellular autophagy. To our knowledge, this is the first report to demonstrate that components of the autophagic pathway are required for formation of a viral replication complex and for efficient viral growth. The autophagy induced by MHV infection was not susceptible to 3-MA treatment, despite 3-MA inhibition of viral yield by up to 86% (data not shown), suggesting that either an alternative pathway of autophagy induction is activated by MHV infection or that viral proteins, insensitive to 3-MA treatment, may replace or complement autophagic pathways. The mechanism by which MHV induces autophagy remains to be determined. Protein kinase R activation has been shown to be essential for autophagic activity (3). Because double-stranded RNA is known to be a potent stimulator of protein kinase R, it is possible that double-stranded RNA generated during viral replication may activate protein kinase R and stimulate autophagy. An alternative possibility is that binding of MHV to the cellular receptor, CEACAM-1, may induce signaling events that result in autophagy.

Viral infection was not able to induce autophagy in *APG5*−/− (A11) cells, indicating that the proteins necessary for autophagic vacuole formation are required for MHV-induced autophagy. The lack of double membrane vesicles in MHV-infected A11 cells was particularly interesting in light of the ability of MHV to replicate in these cells, albeit to reduced levels. This result strongly suggests that DMV formation may not be required for viral replication. However, viral growth was decreased by >99% in the *APG5*−/− cell lines, A11 and B22,

compared with wild-type, *APG5*-expressing R1 cells, and *APG5* knockout cells reconstituted with an Apg5-expressing plasmid (WT13), suggesting that the efficiency of replication is greatly enhanced by DMV formation. The predominant feature of infected A11 cells was the hyper-swollen RER present in these cells that appeared to contain multiple vesicles. Many of these vesicles were surrounded by RER and had the appearance of normal cytoplasm and therefore may have been protrusions of cytoplasm through the cisterna of the swollen ER that gave the appearance of vesicles when viewed in thin section. Alternatively, it is possible that the RER may sequester areas of the cytoplasm. The swollen ER phenotype is similar to the appearance in cells with a defect in ER export function; however, Apg5 is not known to play any role in ER export. RER swelling was only seen in MHV-infected A11 cells and not in mock-infected A11 cells or in infected R1 or DBT cells, suggesting that MHV is specifically interacting with or modulating a process that requires Apg5.

The precise mechanism by which coronaviruses form replication complexes has not been determined. Several recent reports have shown that multiple MHV replicase proteins contain extensive hydrophobic domains that mediate their association with membranes (8, 10, 11). The finding that MHV infection of A11 cells results in expansion of the RER and a lack of MHV-induced DMVs suggests that the RER may be the source membranes for formation of viral replication complexes. Furthermore, if the nascent replicase polyprotein is co-translationally inserted into the ER before proteolytic processing, viral proteins could accumulate in the lumen of the ER, particularly if the mechanism by which these proteins are normally removed is deranged. It is interesting to speculate that components of the autophagy pathway are required for formation of double membrane vesicles and that formation of DMVs serves to sequester and concentrate MHV replicase translated on the ER. Although the molecular mechanisms by which MHV interacts with the process of autophagy remain to be elucidated, this report suggests that MHV may have evolved to utilize a preexisting cellular process to maximize replication efficiency.

The determination of the mechanisms of coronavirus cell interaction may be of critical importance in defining the pathogenesis and possible treatment of coronavirus diseases. The recent identification of a new highly pathogenic human coronavirus (SARS-CoV) as the cause of SARS has dramatically highlighted the need to understand coronavirus virus cell interaction and its mechanisms of intracellular replication (13, 33). The significant conservation of replicase gene organization and probable functions of SARS-CoV and MHV replicase proteins further suggests that it will be important to determine whether SARS-CoV also directs and requires autophagy for efficient replication (34). Because inhibition of autophagy results in dramatic diminution of viral growth, viral factors responsible for the induction of autophagy may provide specific targets for the inhibition of virus replication and development of anti-coronavirus therapies for SARS-CoV and other coronaviruses.

Acknowledgments—We thank John Fleming at the University of Wisconsin for providing the J.1.3 and J.3.3 antibodies. We thank Masami Miwa for experimental assistance, and we gratefully acknowledge Beth Levine for helpful discussions and Sarah Brockway and Rachel Graham for critical reading of the manuscript.

REFERENCES

1. Klionsky, D. J., and Emr, S. D. (2000) *Science* **290,** 1717–1721
2. Reggiori, F., and Klionsky, D. J. (2002) *Eukaryot. Cell* **1,** 11–21
3. Talloczy, Z., Jiang, W., Virgin, H. W., IV, Leib, D. A., Scheuner, D., Kaufman, R. J., Eskelinen, E. L., and Levine, B. (2002) *Proc. Natl. Acad. Sci. U. S. A.* **99,** 190–195
4. Liang, X. H., Kleeman, L. K., Jiang, H. H., Gordon, G., Goldman, J. E., Berry, G., Herman, B., and Levine, B. (1998) *J. Virol.* **72,** 8586–8596
5. Pederson, K., van der Meer, Y., Roos, N., and Snijer, E. J. (1999) *J. Virol.* **73,** 2016–2026
6. Suhy, D. A., Giddings, T. H., Jr., and Kirkegaard, K. (2000) *J. Virol.* **74,** 8953–8965
7. Schlegel, A., Giddings, T. J., Ladinsky, M. S., and Kirkegaard, K. (1996) *J. Virol.* **70,** 6576–6588
8. Gosert, R., Kanjanahaluethai, A., Egger, D., Bienz, K., and Baker, S. C. (2002) *J. Virol.* **76,** 3697–3708
9. Shi, S. T., Schiller, J. J., Kanjanahaluethai, A., Baker, S. C., Oh, J. W., and Lai, M. M. (1999) *J. Virol.* **73,** 5957–5969
10. Sims, A. C., Ostermann, J., and Denison, M. R. (2000) *J. Virol.* **74,** 5647–5654
11. Denison, M. R., and Sims, A. C. (2001) *Adv. Exp. Med. Biol.* **494,** 655–661
12. Mizushima, N., Yamamoto, A., Hatano, M., Kobayashi, Y., Kabeya, Y., Suzuki, K., Tokuhisa, T., Ohsumi, Y., and Yoshimori, T. (2001) *J. Cell Biol.* **152,** 657–668
13. Ksiazek, T. G., Erdman, D., Goldsmith, C., Zaki, S. R., Peret, T., Emery, S., Tong, S., Urbani, C., Comer, J. A., Lim, W., Rollin, P. E., Nghiem, K. H., Dowell, S., Ling, A. E., Humphrey, C., Shieh, W. J., Guarner, J., Paddock, C. D., Rota, P., Fields, B., DeRisi, J., Yang, J. Y., Cox, N., Hughes, J., LeDuc, J. W., Bellini, W. J., and Anderson, L. J. (2003) *N. Engl. J. Med.* **348,** 1953–1966
14. Drosten, C., Gunther, S., Preiser, W., Van Der Werf, S., Brodt, H. R., Becker, S., Rabenau, H., Panning, M., Kolesnikova, L., Fouchier, R. A., Berger, A., Burguiere, A. M., Cinatl, J., Eickmann, M., Escriou, N., Grywna, K., Kramme, S., Manuguerra, J. C., Muller, S., Rickerts, V., Sturmer, M., Vieth, S., Klenk, H. D., Osterhaus, A. D., Schmitz, H., and Doerr, H. W. (2003) *N. Engl. J. Med.* **348,** 1967–1976
15. Poutanen, S. M., Low, D. E., Henry, B., Finkelstein, S., Rose, D., Green, K., Tellier, R., Draker, R., Adachi, D., Ayers, M., Chan, A. K., Skowronski, D. M., Salit, I., Simor, A. E., Slutsky, A. S., Doyle, P. W., Krajden, M., Petric, M., Brunham, R. C., and McGeer, A. J. (2003) *N. Engl. J. Med.* **348,** 1995–2005
16. Hegyi, A., and Ziebuhr, J. (2002) *J. Gen. Virol.* **83,** 595–599
17. Hegyi, A., Friebe, A., Gorbalenya, A. E., and Ziebuhr, J. (2002) *J. Gen. Virol.* **83,** 581–593
18. Lu, X., Lu, Y., and Denison, M. R. (1996) *Virology* **222,** 375–382
19. Lu, Y., and Denison, M. R. (1997) *Virology* **230,** 335–342
20. Lu, X., Sims, A. C., and Denison, M. R. (1998) *J. Virol.* **72,** 2265–2271
21. Lu, Y., Lu, X., and Denison, M. R. (1995) *J. Virol.* **69,** 3554–3559
22. Denison, M. R., Spaan, W. J., van der Meer, Y., Gibson, C. A., Sims, A. C., Prentice, E., and Lu, X. (1999) *J. Virol.* **73,** 6862–6871
23. Dong, S., and Baker, S. C. (1994) *Virology* **204,** 541–549
24. Bost, A. G., Carnahan, R. H., Lu, X., and Denison, M. R. (2000) *J. Virol.* **74,** 3399–3403
25. Bost, A. G., Prentice, E., and Denison, M. R. (2001) *Virology* **285,** 21–29
26. Bi, W., Pinon, J. D., Hughes, S., Bonilla, P. J., Holmes, K. V., Weiss, S. R., and Leibowitz, J. L. (1998) *J. Neurovirol.* **4,** 594–605
27. Hirano, N., Ono, K., and Goto, N. (1984) *Nippon Juigaku Zasshi* **46,** 757–760
28. Hirano, N., Fujiwara, K., Hino, S., and Matumoto, M. (1974) *Arch. Gesamte Virusforsch.* **44,** 298–302
29. Kabeya, Y., Mizushima, N., Ueno, T., Yamamoto, A., Kirisako, T., Noda, T., Kominami, E., Ohsumi, Y., and Yoshimori, T. (2000) *EMBO J.* **19,** 5720–5728
30. Kuma, A., Mizushima, N., Ishihara, N., and Ohsumi, Y. (2002) *J. Biol. Chem.* **277,** 18619–18625
31. Kyuwa, S. (1997) *Exp. Anim.* **46,** 311–313
32. Okumura, A., Machii, K., Azuma, S., Toyoda, Y., and Kyuwa, S. (1996) *J. Virol.* **70,** 4146–4149
33. Marra, M. A., Jones, S. J., Astell, C. R., Holt, R. A., Brooks-Wilson, A., Butterfield, Y. S., Khattra, J., Asano, J. K., Barber, S. A., Chan, S. Y., Cloutier, A., Coughlin, S. M., Freeman, D., Girn, N., Griffith, O. L., Leach, S. R., Mayo, M., McDonald, H., Montgomery, S. B., Pandoh, P. K., Petrescu, A. S., Robertson, A. G., Schein, J. E., Siddiqui, A., Smailus, D. E., Stott, J. M., Yang, G. S., Plummer, F., Andonov, A., Artsob, H., Bastien, N., Bernard, K., Booth, T. F., Bowness, D., Czub, M., Drebot, M., Fernando, L., Flick, R., Garbutt, M., Gray, M., Grolla, A., Jones, S., Feldmann, H., Meyers, A., Kabani, A., Li, Y., Normand, S., Stroher, U., Tipples, G. A., Tyler, S., Vogrig, R., Ward, D., Watson, B., Brunham, R. C., Krajden, M., Petric, M., Skowronski, D. M., Upton, C., and Roper, R. L. (2003) *Science* **300,** 1399–1404
34. Snijder, E. J., Bredenbeek, P. J., Dobbe, J. C., Thiel, V., Ziebuhr, J., Poon, L. L., Guan, Y., Rozanov, M., Spaan, W. J., and Gorbalenya, A. E. (2003) *J. Mol. Biol.* **331,** 991–1004